PCCP

Accepted Manuscript

ROYAL SOCIETY OF CHEMISTRY

www.rsc.org/pccp

Journal Name

COMMUNICATION

Access to Aliphatic Protons as Reporters in Non-Deuterated Proteins by Solid-State NMR

Received 00th January 20xx,
Accepted 00th January 20xx

DOI: 10.1039/x0xx00000x

www.rsc.org/

Suresh Kumar Vasa[a], Petra Rovó[a], Karin Giller[a], Stefan Becker[a], Rasmus Linser[a]*

Interactions within proteins, with their surrounding, and with other molecules are mediated mostly by hydrogen atoms. In fully protonated, inhomogeneous, or larger proteins, however, aliphatic proton shifts tend to show little dispersion despite fast Magic-Angle Spinning. 3D correlations dispersing aliphatic proton shifts by their better resolved amide N/H shifts can alleviate this problem. Using inverse second-order cross polarization (iSOCP), we here introduce dedicated and improved means to sensitively link site-specific chemical shift information from aliphatic protons with a backbone amide resolution. Thus, even in cases where protein deuteration is impossible, the approach may enable access to the various aspects of protein function that are reported on by protons.

Hydrogen atoms are strongly involved in atomic contacts mediating the interactions within as well as between molecules in biological processes. The development of methods towards atomic-resolution characterization of hydrogen atoms has thus represented a major appeal in recent structural biology and will be needed for elucidating protein-protein and protein-drug interactions and their dynamics. Solid-state NMR (ssNMR) is well-suited to characterize structural aspects and dynamics of biological macromolecules at the atomic level.[1,2] Biological ssNMR is traditionally based on the detection of heteronuclei and requires large amounts of isotope-labeled protein. However, detection of sparse protons has now successfully been pursued for proton-diluted samples.[3-7] The associated advantages of deuteration have enabled proton-based backbone assignment strategies[8-10], proton-based structure calculation with long-range distance restraints up to > 10 Å[6,11,12], and characterization of dynamics in the absence of strong proton-proton couplings.[13-15] These sensitive methods usually rely on the introduction of amide, methylene or methyl protons or isolated protonated amino acids into otherwise perdeuterated proteins.[15-19]

Proton dilution by deuterons (reducing the deleterious effects of the proton dipolar network) has resulted in high-resolution proton spectra for several proteins even at moderate MAS. Unfortunately, the preparations mostly rely on both, expression of partially deuterated proteins and/or partial back exchange of deuterons against protons. Such deuteration protocols are not viable for many proteins due to no or low expression in *E. coli* and/or the need for unfolding and refolding steps. Accordingly, finding general ways to access proton-derived NMR parameters in non-deuterated solid samples has remained one of the most important challenges for NMR spectroscopy.

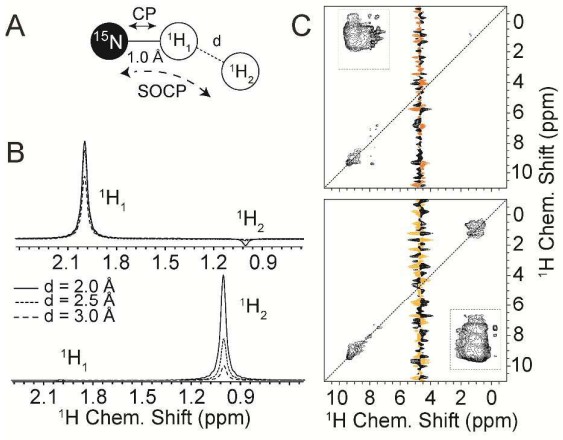

Figure 1. (A) Inverse second-order Cross Polarization (iSOCP). Transfer pathways were approximated using a three-spin system including an amide nitrogen and amide proton coupled to a relayed proton as depicted in A). In B), transfer of magnetization from ^{15}N to proton spins via Hartmann-Hahn CP (upper panel) and iSOCP (lower panel) is depicted as obtained in numerical (SIMPSON) simulations in the absence of off-resonance effects. C) 2D ^{15}N-filtered proton-proton correlation experiments on a non-deuterated, u-^{13}C/^{15}N-labeled micro-crystalline α-spectrin SH3 sample at 55.5 kHz MAS employing SOCP as the first (upper panel) or as the second CP step (iSOCP, lower panel). The diagonal region is represented by a dotted line in the spectra, relayed (aliphatic) correlations are boxed. See the SI for simulation and experimental details.

[a] Max-Planck Institute for Biophysical Chemistry, Department NMR-Based Structural Biology, Am Fassberg 11, 37077 Göttingen
* Corresponding author: *rali@nmr.mpibpc.mpg.de*
Electronic Supplementary Information (ESI) available: [details of any supplementary information available should be included here]. See DOI: 10.1039/x0xx00000x

In case of non-deuterated proteins, proton chemical-shift dimensions have so far been of little use due to broad lines and crowded spectra compared to heteronuclear detection.[20] Recent efforts in probe design now enable MAS of 50-130 kHz, using rotors of 1.3 mm and smaller.[4,9] The development of "ultra-fast MAS" provokes for the first time the use of non-deuterated proteins for proton detection. There are now already a limited number of studies on completely protonated systems demonstrating heteronuclear correlations based on amide proton detection at 60 kHz MAS.[21,22]

Compared with amide protons, aliphatic protons, however, seem to be unattractive for ssNMR under these conditions yet. These protons are highly crowded in CH spectra and at first sight provide a discouraging resolution. The aliphatic H/C correlation (see Supplementary Figure S1B) bears significantly lower resolution than the amide spectrum (see Supporting Figure S1A) due to both, an approximately five times larger number of ^{1}H nuclei and (at 55.5 kHz MAS) slightly wider peak widths. The resolution of aliphatic HC correlations obtained in non-deuterated proteins can potentially be further increased by faster spinning.[3] Given the fact that most protein samples display significantly more intrinsic inhomogeneity than the microcrystalline proteins used in the pioneer studies, a mere reduction of ^{1}H-^{1}H dipolar couplings with all implicated disadvantages, however, may not be a general remedy even at increasing B_0 fields if 2D HC correlations are employed. We show here that MAS speeds achievable with 1.3 mm probes or smaller in combination with amide-dispersed correlations allow access to the sought proton information in the aliphatic region if appropriate spectroscopic strategies are employed.

To make use of the aliphatic proton information despite the residual dipolar linebroadening ($DD_{HH} \approx 130$ kHz) or conformational inhomogeneity, effective dispersing of the aliphatic ^{1}H shifts is required. This can be achieved by correlating these resonances with the better-resolved amide shifts, as it is the case in HN··H spectra based on proton-proton mixing[6,11,12,18] and as can be applied for aliphatic protons[21]. In search for dedicated simple and robust tools to directly access aliphatic proton shifts with an amide HN resolution, we employed SIMPSON[25] simulations of various schemes combined with 2D experimental approaches. Second-order CP (SOCP)[26,27] transfer has been described lately as a three-spin second-order mechanism under low-power conditions, where the presence of a second proton spin is essential for the magnetization transfer from directly bonded protons to a heteronuclear spin. By choosing a proper offset, efficient proton magnetization SOCP can efficiently transfer proton magnetization to a particular region in the carbon spectrum with very low RF power under fast-MAS conditions. Briefly, weak B_1 fields matching the n=0 Hartmann-Hahn conditions are applied on proton and carbon. We find that SOCP, causing similar effective couplings to protons directly coupled to the heteronucleus as to distant protons dipolar coupled to the first ones, can be reversed in direction to achieve a distance-selective magnetization transfer from amide nitrogen to aliphatic protons in a single step. Interestingly, inverse SOCP (iSOCP in the following) allows effective polarization of the distant protons. Both simulations (see Figure 1B and details in the Supplementary Information) as well as their confirmation in NMR experiments (see Figures 1C, S5, and S6) show a predominant magnetization transfer from the amide sites to dipolar-coupled distant protons within roughly 3 Å. The experimental implementation was based on weak, 1-2 ms spin lock of 10-20 kHz B_1 field without use of ramps to transfer ^{15}N magnetization to nearby protons (see the SI for experimental details). To obtain heteronuclear correlations between amide and nearby aliphatic protons, we recorded 3D ^{1}H-^{15}N/^{13}C-^{1}H-correlation spectra using a time-shared pulse sequence with a conventional CP[28] as the first magnetization transfer and an iSOCP as the second transfer (Figure S5).

The time-shared 3D iSOCP experimental scheme provides both, ^{15}N-edited as well as ^{13}C-edited ^{1}H-^{1}H correlations at the same time. Different strips for the ^{15}N-edited and ^{13}C-edited part of the spectrum are shown in Figure 2A and 2B. Usually, the amide nitrogen shows only a weak diagonal peak to its amide proton but cross-peaks to distant protons that are close

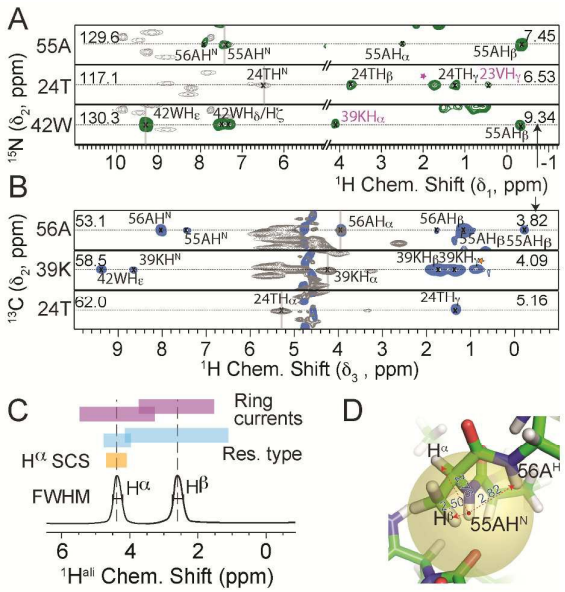

Figure 2. Access to individual proton shifts by 3D $H^{N}N^{H}H^{ali}$ correlations based on inverse SOCP as observed for non-deuterated, u-^{13}C/^{15}N-labeled α-spectrin SH3 micro crystals at 55.5 kHz MAS. Strip plots of (A) ^{15}N- and (B) ^{13}C-edited regions of a time-shared ^{1}H(F_1)-^{15}N/^{13}C(F_2)-^{1}H(F_3) correlation experiment using iSOCP as the second CP transfer. If the Hartmann-Hahn condition is fulfilled, magnetization is predominantly transferred to the relayed proton. The diagonal positions are marked by vertical lines. The spectra are overlaid onto a dipolar-based 2D ^{1}H-^{15}N reference spectrum (in A) and a 2D ^{1}H-^{13}C reference spectrum (in B), respectively (gray). C) Remarkably, if resolved in amide-dispersed strips, the aliphatic protons' linewidths are sufficiently narrow to yield accurate and unambiguously assignable shift information. In addition, this resolution is sufficient to distinguish the variability resulting from different secondary structure (variation within > 0.8 ppm) [30] and residue type (mean values of 4.0 – 4.7 and 1.3 – 4.1 ppm for H^{α} and H^{β}, respectively)[31]. Even in the absence of paramagnetic effects, other influences like ring currents (variation within 2.2 ppm) add to these effects and can increase the distribution of the ^{1}H shifts much further[32], as it is the case for A55. D) Representative distances for signal transfers observed are depicted in the X-ray crystal structure for the 55Ala amide proton (PDB: 2NUZ). The transfers are effective roughly in a range of up to 2.75–3 Å (yellow sphere).

to the corresponding amide proton instead (see Figure 2D). We could achieve assignments of the obtained correlations by the following routine: In the case that cross peaks between amide proton and aliphatic protons appear in both, ^{15}N-edited and ^{13}C-edited strips, the assignment is straightforward and unambiguous. Similar is the case for those resonances that represent well-resolved amide proton and ^{13}C chemical shifts in ^{13}C-edited experiments. In any case, if the cross-peak chemical shift value matches with more than one aliphatic proton chemical shift value, then the distance (from the X-ray structure, 2.5 to 3.5 Å away from amide protons, as can be deduced from the unambiguous peaks) was the criterion for assignment. Contacts obtained and their distances are listed in Table S1 (in the SI). Under the described conditions, using processing parameters optimal for highest resolution, the time-shared iSOCP-based spectra yield a maximum signal to noise of approximately 10:1 within 34 h. This is significantly more sensitive than a combination of back transfer to H^N and successive homonuclear (RFDR[29]) proton-proton mixing (see the SI for details), which – like HN··H experiments using homonuclear ^{1}H-^{1}H mixing schemes generally[11,18] – can be used to yield the same spectral information[21]. Regarding the assignment strategy for unknown structures, the combination of N/C cross-validation and spatial restriction (meaning mostly that the peaks are within the same residue) make an assignment possible. In critical cases, an additional ^{13}C/^{15}N dimension added to the proposed 3D experiment with proton detection could help reduce further ambiguities.

A buildup profile of aliphatic polarization by iSOCP is shown in Figure S10 (SI) for some cases in which cross-peaks are unambiguous already in 2D HN experiments. Such build-up curves may be useful for determination of distance-related information between amide protons and aliphatic protons. A combination of the spectra shown here with RFDR or other recoupling sequences for longer-range contacts and higher-dimensionality (>3D) experiments[5,18] may be helpful to enable protein structure calculation from minimal protein amounts for non-deuterated samples.

Facilitating atom-resolved spectra of aliphatic protons with improved sensitivity, these approaches allow us to demonstrate unambiguous identification and readout of aliphatic proton resonance frequencies in minimal amounts of undeuterated protein. Representative line widths of the individual proton resonances that we obtain in 3D strips resolved by the amide shifts under the experimental conditions amount to approximately 0.2-0.4 ppm. Lowest values of 140 Hz (0.175 ppm) are found for methyl groups. Given the distance-dependent access to aliphatic protons, we mostly obtain H^α and H^β (and sometimes H^γ) proton data in the F1/F2 amide-resolved strips. Shifts of geminal protons attached to the same carbon are mostly degenerate and thus cannot be distinguished. On the other hand, residue-type-specific shielding parameters, secondary structure, and other influences, which can have even stronger effects, easily induce shifts significantly larger than the aliphatic HWFM.[30] In line with what can be derived from previous work[21], this fact represents a basis for the utility of protons as a carrier of local chemical information.

Typical aliphatic proton shifts for different amino acid types scatter over large ranges within the same nucleus type (Figure 2C). For example, H^α mean values vary from 4.0 – 4.7 and H^β values from 1.3 – 4.1 ppm (BMRB data bank).[31] The differences in the H^α/H^β patterns expected for different residue types provide a means to sensitively assess the kind of amino acid present at a specific position. This is commensurate to the typical carbon chemical shifts for different amino acid types and provides a complementary tool for sequential resonance assignments in proteins. See a list of the aliphatic shifts in the SH3 domain in comparison with random coil values for comparison in Table S2 of the SI.

The access to non-exchangeable protons is also able to inform on local magnetic fields and individual shielding parameters. Since most through-space effects on the chemical shift like intra- and intermolecular protein interactions are fully or partly elicited by aliphatic contacts, their facilitated NMR accessibility thus provides a reporter of protein-protein contacts or protein-small molecule interactions.[32] This potential is represented in Figure 3C/D and Figure S11 (Supplementary Material), depicting chemical shifts in the individual SH3 domain aliphatic protons relative to their random coil chemical shifts. Deviations from random-coil values clearly exist, reflecting for example whether a side chain is or is not in contact with other protein structural elements: Water-exposed side chains like W41 and W42 do not show significant difference values (<0.2 ppm for all protons).

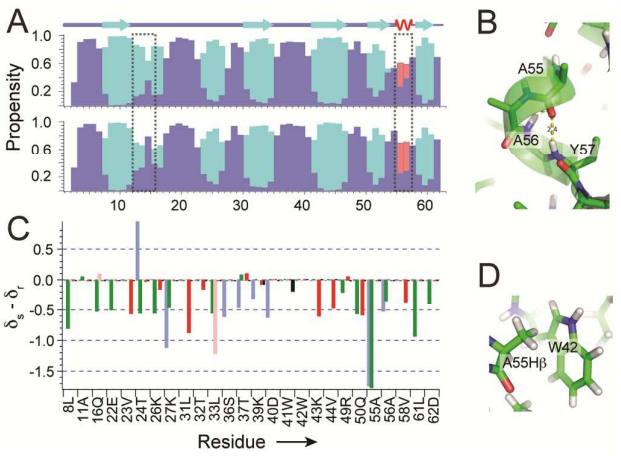

Figure 3. Comparison of predicted secondary structure in the SH3 domain without (top) and with (below) consideration of proton chemical shifts. The data was generated using TALOS+. Heteronuclear chemical shifts and proton chemical shifts had been published previously.[1] Cyan, red, and blue colors represent the propensity of an amino acid to be in β-sheet, α-helix and loop conformation, respectively. Secondary structure from the X-ray structure is shown on top, regions with improved prediction are boxed. (B) The α-helical stretch (right box in A) is evident in the crystal structure. (C) Deviation of observed chemical shifts for aliphatic protons in the solid state (blue: H^α, green: H^β, red, light red: Hγ, black: Hδ) from random-coil chemical shift values. A55 proton shifts clearly report on the proximity to the aromatic W42. (D) Structural representation of the A55 environment.

On the other hand, for example, 55Ala aliphatic chemical shifts are extremely up-field shifted relative to random coil due to neighboring ring-current effects (>1.5 ppm for both H^{α} and H^{β}). Aliphatic hydrogens as exposed reporter nuclei will be more useful for mapping such interactions than amide protons, whose chemical shifts are mostly determined by their hydrogen bonds, and than heteronuclei, whose sensitivity to environmental shielding is less pronounced due to their more protected residence and lower gyromagnetic ratio.[32]

^{1}H chemical-shift information of aliphatic side chain groups also reports on secondary structure, which causes variations of H^{α} shifts within 0.8 ppm: With respect to random coil, H^{α} resonances are shifted by approximately 0.4 ppm up or down for helical or strand structure, respectively.[30,32] Proton shifts can thus also be exploited for secondary-structure assessment (e. g., TALOS[33]) in terms of secondary chemical shifts (see Figure 3A/B). Indeed, in the SH3 domain, secondary-structure prediction by TALOS+[33] is significantly improved for parts of the protein upon including the H^{N}, H^{α} and H^{β} chemical shift information content in addition to heteronuclear shifts only: When only heteronuclear shifts are used as an input for the TALOS program, in the short helical region (55Ala-56Ala), only a 20 % helix probability is predicted for A56. Upon inclusion of proton chemical shifts, the correct structure is predicted with a propensity of 41 %. Similarly, the propensity of the loop 12Leu-16Gln, which achieves the correct 'loop' prediction with only 19 % probability on average based on heteronuclear shifts only, is improved to 46 % upon inclusion of proton secondary chemical shifts. The other regions are predicted correctly with or without ^{1}H shift information. The helical stretch is a critical part of the protein structure due to its biological role in recognizing Pro-rich sequences in its binding partners. The one-turn helix is not usually recognized correctly by angle-based algorithms like in crystallographic structure viewing programs, despite the fact that crystallography clearly shows a helical pattern held in place by the usual *i* to *i+4* H-bond structure. Similarly to secondary chemical shift data and local chemical variables, many other biologically relevant parameters can be obtained from aliphatic protons as abundant and exposed reporters. This large versatility has been amply demonstrated in solution NMR studies and can logically be transferred to solid-state NMR. For example, binding of small molecules to protein surfaces has a known effect on aliphatic hydrogen resonances.[32,35] Characterization of contacts elucidated by paramagnetic relaxation enhancement[36,37] or contact shifts will now be applicable to the entire set of reporting spins in a protein without deuteration. Using these approaches, water accessibility measurements based on magnetization transfer by water-to-protein proton NOE[38-40] is another straightforward application. New perspectives arise to characterize local mobility – as for example derived from HC dipolar couplings[15] – or to obtain distance restraints via latest protein structure determination schemes[41]. Most of these possibilities have been demonstrated for H^{N} in deuterated proteins and can now be expanded to the aliphatic side chains in fully protonated proteins.

To conclude, we have shown that improved access to aliphatic proton chemical shifts even in the case of a non-deuterated protein can be obtained using inverse-Second-Order-CP-based 3D correlations. Aliphatic shifts can be accessed and assigned from minimal protein amounts by a combination of ultrafast Magic Angle Spinning and iSOCP transfer techniques that correlate the resonances of non-exchangeable protons with their better-resolved and usually clearly assigned amide shifts. We have demonstrated that protons generally bear rich information content and are amenable to report on residue type, atomic contacts, and secondary structure. A plethora of further uses of proton shift accessibility can be derived from solution NMR and previous studies using amides in deuterated solid proteins. These possibilities will be of high value for the characterization of eukaryotic membrane proteins and other targets difficult to express in *E. coli*, which represent increasingly important candidates for structural biology studies.

Acknowledgements

We are thankful to Brigitta Angerstein and Dr. Dirk Bockelmann for technical assistance. RL acknowledges support from the Max-Plank Gesellschaft, from the Deutsche Forschungsgemeinschaft (SFB 803, project A04, and an Emmy Noether fellowship), and the Verband der Chemischen Industrie (VCI) in terms of a Liebig junior group fellowship.

References

1 F. Castellani, B. J. van Rossum, A. Diehl, M. Schubert, K. Rehbein, H. Oschkinat, *Nature* **2002**, *420*, 98.
2 S. H. Park, B. B. Das, F. Casagrande, Y. Tian, H. J. Nothnagel, M. Chu, H. Kiefer, K. Maier, A. A. De Angelis, F. M. Marassi, S. J. Opella, *Nature* **2012**, *491*, 779.
3 J. M. Lamley, D. Iuga, D. C. Öster, H. J. Sass, M. Rogowski, A. Oss, J. Past, A. Reinhold, S. Grzesiek, A. Samoson, J. R. Lewandowski, *J. Am. Chem. Soc.* **2014**, *136*, 16800.
4 V. Agarwal, S. Penzel, K. Szekely, R. Cadalbert, E. Restori, A. Oss, J. Past, A. Samoson, M. Ernst, A. Böckmann, B. H. Meier, *Angew. Chem. Int. Ed.* **2014**, *53*, 12253.
5 R. Linser, B. Bardiaux, L. B. Andreas, S. G. Hyberts, V. K. Morris, G. Pintacuda, M. Sunde, A. H. Kwan, G. Wagner, *J. Am. Chem. Soc.* **2014**, *136*, 11002.
6 M. J. Knight, A. J. Pell, I. Bertini, I. C. Felli, L. Gonnelli, R. Pierattelli, T. Herrmann, L. Emsley, G. Pintacuda, *Proc. Natl. Acad. Sci. U.S.A.* **2012**, *109*, 11095.
7 S. Asami, P. Schmieder, B. Reif, *J. Am. Chem. Soc.* **2010**, *132*, 15133.
8 R. Linser, M. Dasari, M. Hiller, V. Higman, U. Fink, J. M. Lopez del Amo, S. Markovic, L. Handel, B. Kessler, P. Schmieder, D. Oesterhelt, H. Oschkinat, B. Reif, *Angew. Chem., Int. Ed.* **2011**, *50*, 4508.
9 E. Barbet-Massin, A. J. Pell, J. S. Retel, L. B. Andreas, K. Jaudzems, W. T. Franks, A. J. Nieuwkoop, M. Hiller, V. Higman, P. Guerry, A. Bertarello, M. J. Knight, M. Felletti, T. Le Marchand, S. Kotelovica, I. Akopjana, K. Tars, M. Stoppini, V. Bellotti, M. Bolognesi, S. Ricagno, J. J. Chou, R.G. Griffin, H. Oschkinat, A. Lesage, L. Emsley, T. Herrmann, G. Pintacuda, *J. Am. Chem. Soc.* **2014**, *136*, 12489.
10 R. Linser, U. Fink, B. Reif, *J. Am. Chem. Soc.* **2010**, *132*, 8891.
11 R. Linser, B. Bardiaux, V. Higman, U. Fink, B. Reif, *J. Am. Chem. Soc.* **2011**, *133*, 5905.

12 D. H. Zhou, J. J. Shea, A. J. Nieuwkoop, W. T. Franks, B. J. Wylie, C. Mullen, D. Sandoz; C. M. Rienstra, *Angew. Chem., Int. Ed.* **2007**, *46*, 8380.
13 V. Chevelkov, U. Fink, B. Reif, *J. Am. Chem. Soc.* **2009**, *131*, 14018.
14 P. Schanda, B. H. Meier, M. Ernst, *J. Am. Chem. Soc.* **2010**, *132*, 15957.
15 S. Asami, J. R. Porter, O. F. Lange, B. Reif, *J. Am. Chem. Soc.* **2015**, *137*, 1094.
16 R. Linser, V. Chevelkov, A. Diehl, B. Reif, *J. Magn. Reson.* **2007**, *189*, 209.
17 V. Chevelkov, K. Rehbein, A. Diel, B. Reif, *Angew. Chem., Int. Ed.* **2006**, *45*, 3878.
18 M. Huber, S. Hiller, P. Schanda, M. Ernst, A. Böckmann, R. Verel, B. H. Meier, *Chem. Phys. Chem.* **2011**, *12*, 915.
19 D. Mance, T. Sinnige, M. Kaplan, S. Narasimhan, M. Daniëls, K. Houben, M. Baldus and M. Weingarth, *Angew. Chem. Int. Ed.*, **2015**, doi: 10.1002/anie.201509170.
20 C. M. Guo, G. J. Hou, X. Y. Lu, B. O'Hare, J. Struppe, T. Polenova, *J. Biomol. NMR* **2014**, *60*, 219.
21 A. Marchetti, S. Jehle, M. Felletti, M. J. Knight, Y. Wang, Z. Q. Xu, A. Y. Park, G. Otting, A. Lesage, L. Emsley, N. E. Dixon, G. Pintacuda, *Angew. Chem., Int. Ed.* **2012**, *51*, 10756.
22 D. H. Zhou, G. Shah, M. Cormos, C. Mullen, D. Sandoz, C. M. Rienstra, *J. Am. Chem. Soc.* **2007**, *129*, 11791.
23 R. Verel, M. Ernst, B. H. Meier, *J. Magn. Reson.* **2001**, *150*, 81-89.
24 S. Xiang, K. Grohe, P. Rovó, S. K. Vasa, K. Giller, S. Becker, R. Linser, *J. Biomol. Nmr,* **2015**, *62*, 303.
25 M. Bak, J. T. Rasmussen, N. C. Nielsen, N. C. *J. Magn. Reson.* **2000**, *147*, 296.
26 A. Lange, I. Scholz, T. Manolikas, M. Ernst, B. H. Meier, *Chem. Phys. Lett.* **2009**, *468*, 100.
27 V. Vijayan, J. P. Demers, J. Biernat, E. Mandelkow, S. Becker, A. Lange, *Chem. Phys. Chem.* **2009**, *10*, 2205.
28 M. Baldus, B. H. Meier, *J. Magn. Reson.* **1997**, *128*, 172.
29 A. E. Bennett, J. H. Ok, R. G. Griffin, S. Vega, *J. Chem. Phys.* **1992**, *96*, 8624.
30 L. Szilágyi, *Prog. Nucl. Mag. Res.* **1995**, *27*, 325.
31 E. L. Ulrich, *Nucleic Acids Res.* **2008**, *36*, D402.
32 M. P. Williamson, *Prog. Nucl. Mag. Res.* **2013**, *73*, 1.
33 Y. Shen, F. Delaglio, G. Cornilescu, A. Bax, *J. Biomol. Nmr,* **2009**, *44*, 213.
34 J. T. Nguyen, C. W. Turck, F. E. Cohen, R. N. Zuckermann, W. A. Lim, Science, 1998, 282, 2088-2092.
35 M. A. Mccoy, D. F. Wyss, *J. Am. Chem. Soc.* **2002**, *124*, 11758.
36 A. Krushelnitsky, E. deAzevedo, R. Linser, B. Reif, K. Saalwächter, D. Reichert, *J. Am. Chem. Soc.* **2009**, *131*, 12097.
37 G. Pintacuda, G. Otting, *J. Am. Chem. Soc.* **2002**, *124*, 372.
38 N. V. Nucci, M. S. Pometun, A. J. Wand, *Nat. Struct. Mol. Biol.* **2011**, *18(2)*, 245.
39 G. Otting, E. Liepinsh, K. Wuthrich, *Science* **1991**, *254*, 974.
40 V. Chevelkov, K. Faelber, A. Diehl, U. Heinemann, H. Oschkinat, B. Reif, *J. Biomol. NMR,* **2005**, *31*, 295.
41 R. Linser, B. Bardiaux, S. G. Hyberts, A. H. Kwan, V. K. Morris, M. Sunde and G. Wagner, *J. Am. Chem. Soc.*, **2014**, *136*, 11002–11010.